RADIAL TURBOFAN CFD ANALYSIS

João Roberto Barbosa
Edson Luiz Zaparoli
Cláudia Regina de Andrade
Instituto Tecnológico de Aeronáutica, Divisão de Engenharia Mecânica, Praça Marechal Eduardo Gomes, 50, Vila das Acácias, CEP 12228-900, São José dos Campos, SP

Nelson Manzanares Filho
Waldir de Oliveira
Genésio José Menon
Ramiro Gustavo Ramirez Camacho
Universidade Federal de Itajubá, Instituto de Engenharia Mecânica, Av. BPS, 1303, bairro Pinheirinho, Itajubá - MG

Abstract
At this work the airflow in a radial turbofan was numerically studied. Geometric data extracted from the experimental test rig developed by Oliveira (2001) were used to build an accurate CAD model reproducing all details required to a reliable computational simulation. For the numerical solution, a finite volume method to solve the governing equations (mass, momentum and turbulence model) in a rotating reference frames approach was employed. The fan moving parts render the problem unsteady when viewed from a stationary frame. Using rotating reference frames, however, the flow around the moving part can be modeled as a steady-state problem with respect to the moving frame. The discretized equations system for pressure and velocity component is iteratively solved using a pressure based formulation (SIMPLE segregated algorithm). Numerical and experimental results were compared for different volumetric flow rate. After numerical solution validation, CFD post-processing tools are used to evaluate rotor internal airflow intending equipment performance improvement.

1. Introduction

Centrifugal turbomachines are widely used for their ability to generate relatively high pressure ratios for each stage. They are often found in gas turbine engines, heating, ventilation, and air conditioning systems, radial turbofans and pumps, (Choi et al, 2003). Most past flowfield studies were motivated mainly by interest in producing improved radial turbofan performance using both experimental tests and/or CFD tools.

Oliveira (2001) performed an experimental study in radial turbomachines employing a specific test rig without irregular external interference on the airflow. A measuring system based on an aerodynamic probe located in the centrifugal impeller outlet was used to evaluate flow characteristics. Author provided results for pressure rise coefficient as a function of the flow coefficient.

Younsi et al. (2007) studied numerically the impeller-volute interaction of a centrifugal fan. 3D-unsteady calculations using the Unsteady Reynolds Averaged Navier-Stokes (URANS) approach has been applied on the computational domains which have been divided into two zones, a rotating zone including the impeller and a stationary zone including the volute interactions and unsteadiness induced by the motion of rotating blades relatively to the volute. The overall behavior of the fan has been validated experimentally at different flow rates.

Gašparovič and Čarnogurská (2008) performed an aerodynamic optimization of a centrifugal fan casing using CFD tool. The authors obtained results of flow field in both outlets, and subsequently to optimize the shape of casing in order to homogenize flow field in outlets assuming that mass flow through outlets is preserved.

Karanth and Sharma (2009) analyzed the effect of a radial gap on impeller-diffuser flow interaction as well as on the flow characteristics of a centrifugal fan. They used a numerical methodology involving moving mesh technique to predict the real flow behavior, as exhibited when a target blade of the impeller is made to move past corresponding vane on the diffuser. Their results showed that (i) the static pressure recovery and total pressure loss for the diffusing components of the fan change with the radial gap and (ii) the overall efficiency also found to increase for relatively larger gap.

At the present work, the radial turbofan performance characteristics will be determined from the total pressure difference between the impeller discharge and its inlet, at various flow rates. The mathematical model equations for a rotating reference frame are solved employing the finite volume method. To validate the numerical procedure, CFD results are compared with experimental data (Oliveira, 2001). Hence, the radial turbofan efficiency is also calculated for a constant rotor speed of rotation.

2. Mathematical Formulation

The flow in a radial turbomachine is essentially unsteady, but under overall stable conditions, a steady-state moving reference frame (MRF) model can be used. This technique can solve problems typically involving moving parts

(such as rotating blades, impellers, and similar types of moving surfaces), and it is the flow around these moving parts that is of interest. At this approach, the governing equations must incorporate the additional acceleration terms which occur due to the transformation from the stationary to the rotating reference frame.

At the present work, the rotor domain was modeled using the moving reference frame (MRF) model, with constant rotational speed, while the inlet and outlet ducts domain was assumed to be stationary, Fig (1).

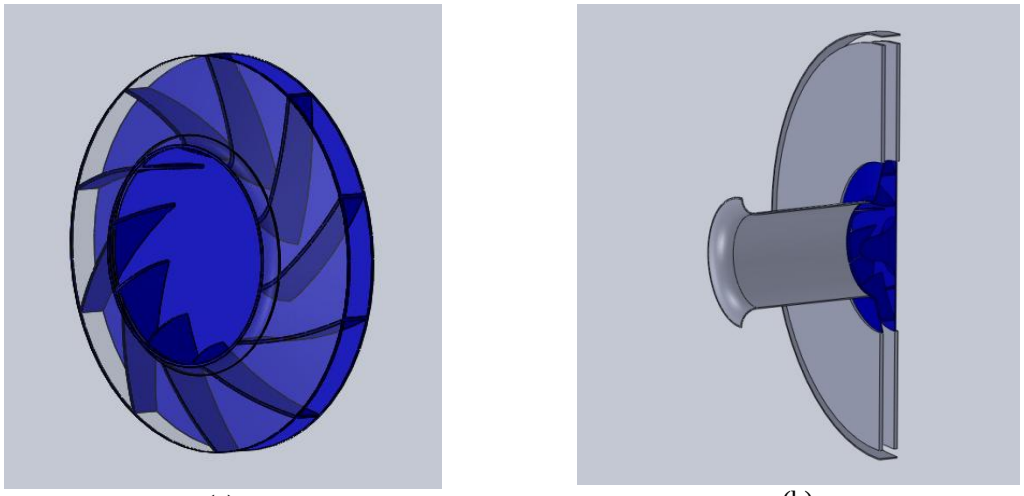

(a) (b)

Figure 1. CAD model: (a) rotor with 10 circular arc blades; (b) radial fan cross-section.

In a rotating reference frame with constant angular velocity ($\boldsymbol{\omega}$), the relative velocity ($\boldsymbol{v_r}$) can be obtained as:

$$\boldsymbol{v_r} = \boldsymbol{v} - \boldsymbol{u_r} \tag{1}$$

with:

$$\boldsymbol{u_r} = \boldsymbol{\omega} \times \boldsymbol{r} \tag{2}$$

where:, $\boldsymbol{v}$ is the absolute velocity; $\boldsymbol{u_r}$ is the "whirl" velocity (due to the moving frame system) and $\boldsymbol{r}$ is the position-vector.

Employing the relative velocity approach, the governing equations (mass and momentum conservation) for a constant $\boldsymbol{\omega}$ rotating frame can be written as follows:

$$\frac{\partial \rho}{\partial t} + \nabla \cdot (\rho \boldsymbol{v_r}) = 0 \tag{3}$$

and

$$\frac{\partial (\rho \boldsymbol{v_r})}{\partial t} + \nabla \cdot (\rho \boldsymbol{v_r} \boldsymbol{v_r}) + \rho(2\boldsymbol{\omega} \times \boldsymbol{v_r} + \boldsymbol{\omega} \times \boldsymbol{\omega} \times \boldsymbol{r}) = -\nabla p + \nabla \cdot \overline{\overline{\tau_r}} \tag{4}$$

Note that the momentum equation contains two additional acceleration terms: the Coriolis acceleration ($2\omega \times v_r$) and the centripetal acceleration ($\omega \times \omega \times r$). Besides, the viscous stress term is $\left(\overline{\overline{\tau_r}}\right)$ identical to the stationary frame formulation, except that relative velocity derivatives are used, resulting that:

$$\overline{\overline{\tau_r}} = \mu_{eff} \left[\nabla \boldsymbol{v_r} + (\nabla \boldsymbol{v_r})^{\,\mathrm{tr}} - \frac{\mathbf{2}}{\mathbf{3}} (\nabla \cdot \boldsymbol{v_r}) \boldsymbol{I} \right] \tag{5}$$

where μ_{eff} is the effective viscosity (laminar + turbulent), tr indicates de transpose, I is the unit tensor, and the second term on the right hand of Eq. (5) is the effect of volume dilation

The effects of turbulence were modeled using the realizable k-ε turbulence model with non-equilibrium wall functions (Fluent Inc., 2010). The working fluid (air) was assumed to be incompressible with constant properties.

To reduce the computational effort, periodic boundary conditions were imposed at successive fan-blade mid-surfaces as indicated in Fig (2). Using this procedure, the flow quantities are calculated on the angular slice surrounding each blade, instead of the entire airflow domain depicted in Fig. (1).

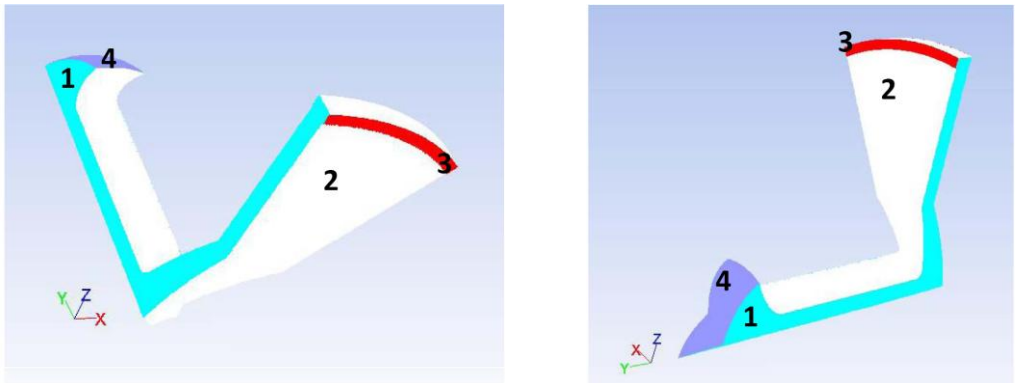

Figure 2. Computational flow domain and boundary conditions: 1 – periodic; 2 – wall; 3 - pressure outlet and 4 – mass flow inlet.

The differential partial equations employed to take account the turbulence effect (realizable k-ε model) require two parameters at the inlet surface (4): the intensity level (10%) and the turbulent-to-laminar viscosity ratio ($\mu_{tur}/\mu_{lam} = 10$).

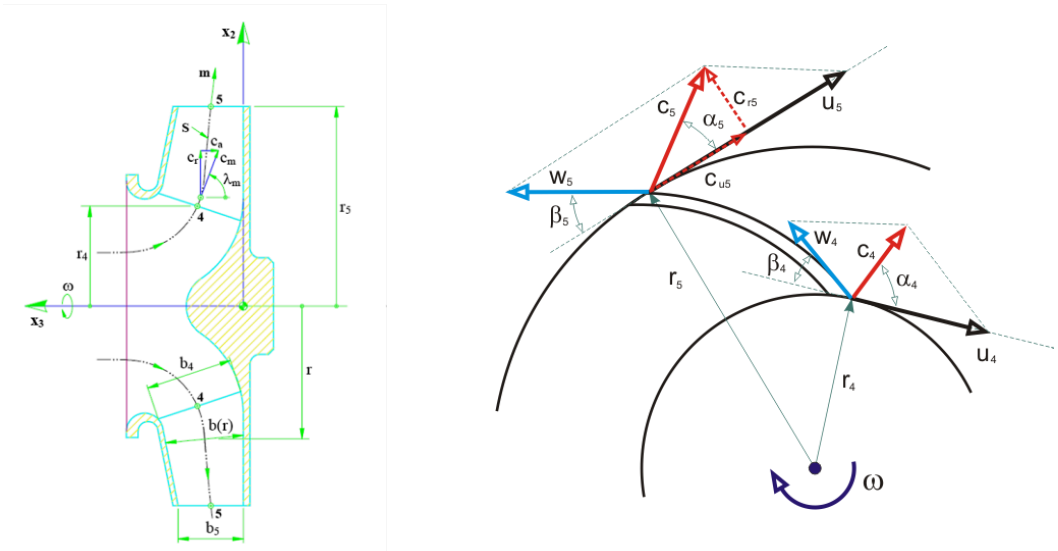

(a) (b)

x_2, x_3 = orthogonal axis system, ω = angular velocity, r_4 = blade inlet radius, r_5 = blade outlet radius, b_4 = blade inlet width, b_5 = blade outlet width, u_5 = blade tangential velocity, c_5 = fluid absolute velocity and w_5 = fluid relative velocity.

Figure 3. (a) Radial turbofan: rotor nomenclature (Oliveira, 2001); (b) Velocity triangles.

At the present work, numerical results are compared with experimental ones following the nomenclature indicated in Figure 3 and are expressed by two non-dimensional parameters: the flow coefficient (ϕ) and the total pressure rise coefficient (ψ) given by:

$$\phi = \frac{\left(\frac{Q}{2\pi r_5 b_5}\right)}{\omega r_5} = \frac{c_{r5}}{u_5} \tag{6}$$

where Q is the volumetric flow rate [m^3/s], c_{r5} is the radial absolute velocity at impeller exit and u_5 is the tangential velocity at impeller exit.

$$\psi = \frac{2 \cdot Y}{(\omega r_5)^2}, \quad Y = \frac{\Delta p_t}{\rho} \tag{7}$$

where Y is the specific work [kJ/kg], ρ is the fluid density [kg/m^3] and Δp_t is the actual total pressure rise [Pa] between fan outlet and inlet sections, respectively.

The actual total pressure rise is less than the ideal total pressure rise ($\Delta p_{t,i}$) which can be calculated as:

$$\Delta p_{t,i} = \rho\, u_5 \left[u_5 - c_{r5} \cot(\beta_5) \right] = \rho (u_5)^2 \left[1 - \phi \cot(\beta_5) \right] \quad (8)$$

The radial fan efficiency (η) is defined as:

$$\eta = \frac{\Delta p_t}{\Delta p_{t,i}} = \frac{\Delta p_t}{\rho (u_5)^2 \left[1 - \phi \cot(\beta_5) \right]} \quad (9)$$

Following the experimental work, the herein results were obtained with a constant fan angular velocity (ω), Fig. (3).

3. Solution Methodology

The mathematical model equations are treated by finite volume method employing second order discretization for convective terms. The SIMPLE algorithm is used to pressure-velocity coupling. A tetrahedric body-fitted mesh is generated inside the airflow domain as shown in Fig. 4.

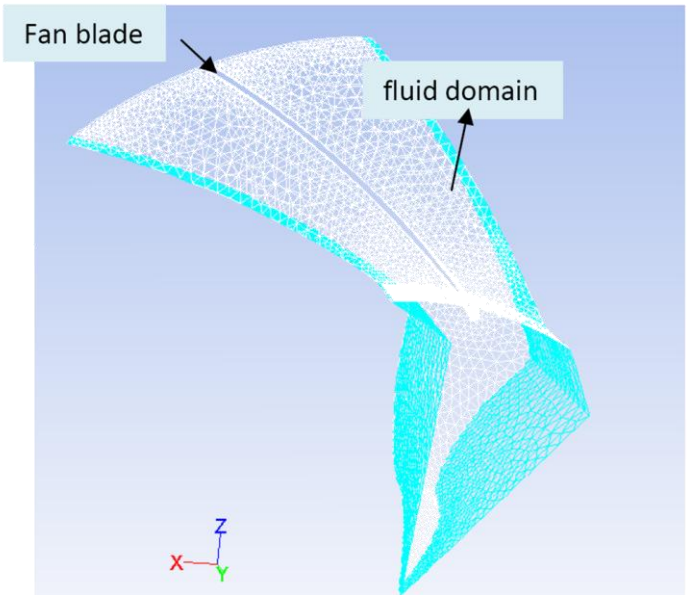

Figure 4. Rotor slice mesh.

The steady-state MRF approach is used to simulate centrifugal fan rotational effects. The rotating axis is parallel to y-axis with a pre-specified angular velocity (ω = 314.16 rad/s; n = 50 rps).

4. Results

In order to validate the numerical tool, CFD results are compared with experimental ones. Figure 5 presents the pressure rise coefficient as a function of the flow coefficient (employing Eq. 6 and Eq. 7). At higher ϕ values, there is a good agreement while at lower flow coefficient numerical results overpredict experimental values. This fact can be probably attributed to secondary flow loss which is not captured by the mesh when detachment occurs at the blade suction side (as shown in Figure 6a, for the relative velocity magnitude distribution at ϕ = 0.2).

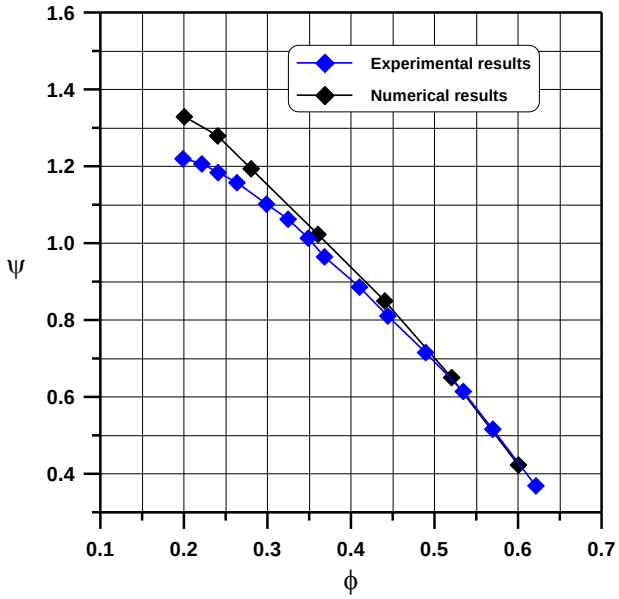

Figure 5. Total pressure rise coefficient results for fan rotor.

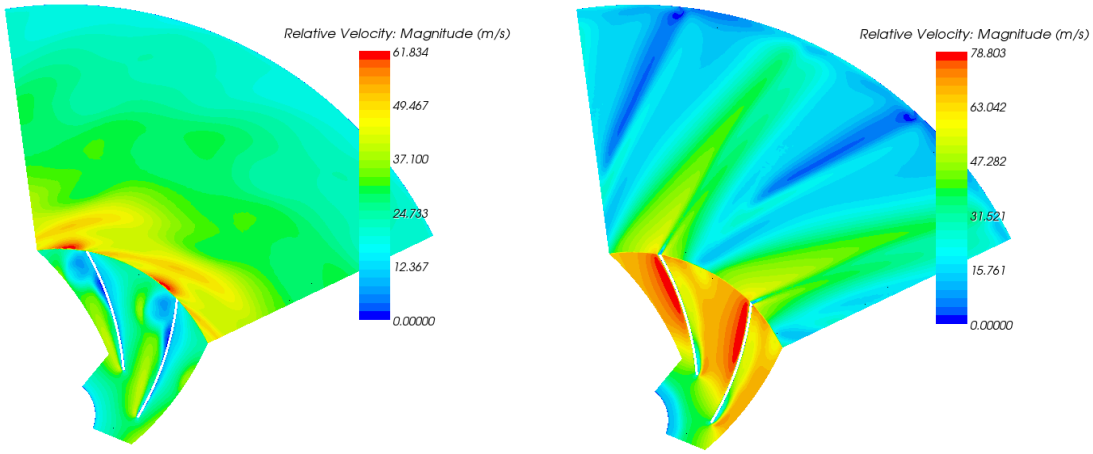

(a) ϕ = 0.2 (b) ϕ = 0.6

Figure 6. Relative velocity magnitude ($\boldsymbol{v_r}$) distribution.

When the radial turbofan volumetric flow rate is too much below the design-point value, the airflow pattern exhibits intense rotational speed inside the diffuser, Fig. 6(a). On the other hand, at higher flow rates, the radial airflow fills the whole blade channel, Fig. 6(b) and the air flows more radially at the diffuser domain. At this last case (ϕ = 0.6), numerical and experimental showed a better agreement as illustrates Fig. 5.

Numerical and experimental results for the radial turbofan efficiency (Eq. 9) as a function of the flow coefficient are plotted in Figure 7. Note that a maximum efficiency occurs close to ϕ = 0.25, which is captured by the simulation although it is overpredicted.

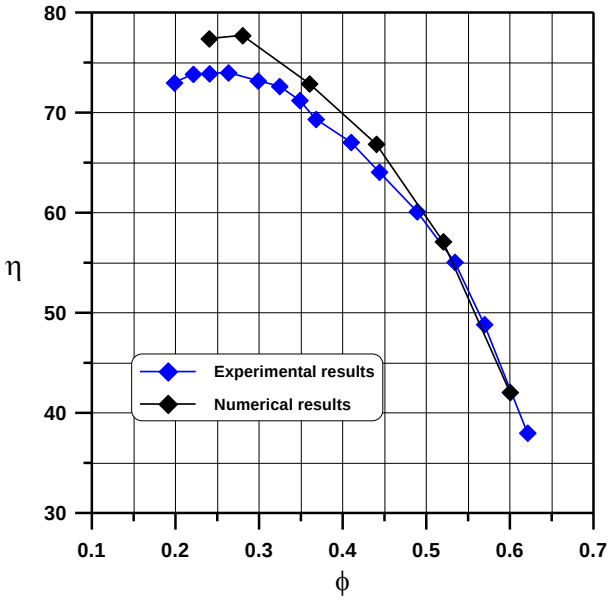

Figure 7. Radial turbofan efficiency (η) as a function of the flow coefficient (ϕ).

Numerical results fit better with experimental ones at higher flow coefficient values as already verified for total pressure rise coefficient results (Fig. 5).

5. Final Remarks

At the present work, the radial turbofan flow was numerically studied employing a finite volume technique to solve the rotating reference frame RANS equations under a constant rotor speed. Numerical results agree well with experimental ones at higher flow coefficient (ϕ) values, both for total pressure rise and fan efficiency. This discrepancy can be attributed to the more intense tangential velocity patterns at lower flow coefficient values (Fig. 6).

6. Acknowledgments

Authors are grateful to CAPES (Coordenação de Aperfeiçoamento de Pessoal de Nível Superior) by the support to development of this work (ITA-UNIFEI PROCAD project, grant #23038.023930/2008-75).

7. References

Choi, J. S., McLaughlin, D. K. and Thompson, D. E., 2003, "Experiments on the unsteady flow field and noise generation in a centrifugal pump impeller", Journal of Sound and Vibration, Vol. 263, pp.493-514.

Gašparovič, P. and Čarnogurská, M., 2008, "Aerodynamic Optimisation of Centrifugal Fan Casing Using CFD", Journal of applied science in the thermodynamics and fluid mechanics, Vol. 2 (1).

Karanth, K.V. and Sharma, N.Y., 2009, "CFD Analysis on the Effect of Radial Gap on Impeller-Diffuser Flow Interaction as well as on the Flow Characteristics of a Centrifugal Fan", International Journal of Rotating Machinery, doi:10.1155/2009/293508.

Oliveira, W., 2001. "Análise do Escoamento em Turbomáquinas Radiais", Tese de Doutorado, Instituto Tecnológico de Aeronáutica, 264 p.

Younsi M., Bakir F., Kouidri S. and Rey R., 2007, "3D Unsteady Flow in a Centrifugal Fan: Impeller - Volute Interaction", Journal of Computational and Applied Mechanics, Vol. 8 (2)., pp. 211–223.

8. RESPONSIBILITY NOTICE

The authors are the only responsible for the printed material included in this paper.